Transportation Geotechnics 51 (2025) 101499

Contents lists available at ScienceDirect

Transportation Geotechnics

journal homepage: www.elsevier.com/locate/trgeo

Laboratory model test of contact erosion in railway substructure

Shaoheng Dai [a], Xuzhen He [a], Feng Gao [b,*], Wenhua Zhong [c], Yewei Zheng [d], Sheng Zhang [e,f,*]

[a] School of Civil and Environmental Engineering, University of Technology Sydney, Ultimo, NSW 2007, Australia
[b] School of Traffic and Transportation Engineering, Changsha University of Science & Technology, Changsha, 410114, Hunan, China
[c] Qinghai Communications Holding Group Co., Ltd, Xining, Qinghai 810000, China
[d] School of Civil Engineering, Wuhan University, Wuhan, Hubei 430072, China
[e] School of Civil Engineering, Central South University, Changsha 410075, China
[f] School of Civil Engineering, Qinghai University, Xining 810016, China

ARTICLE INFO

Keywords:
Contact erosion
Railway substructure
Cyclic loading
Hydraulic gradient
Particle migration

ABSTRACT

The underestimated risk of contact erosion failure in railway substructures poses a significant threat to railway safety, particularly at the interface between the ballast/subballast and subgrade. The larger constriction size at this interface exacerbates the potential for long-term erosion, necessitating attention to safeguard railway integrity. This study introduces a novel laboratory erosion testing apparatus to evaluate contact erosion at the subballast-subgrade interface under cyclic loading. Subgrade soils with varying fines contents are tested, and the effect of pressure head on erosion is investigated in detail. The results indicate that sandy soil with higher internal stability exhibits a higher critical pressure head for contact erosion. Cyclic loading induces oscillations in pore water pressure within the subballast layer, with higher pressure heads leading to larger amplitudes. Excess pore water pressure is generated in the sandy soil layer during cyclic loading and gradually dissipates over time. Fine eroded particles migrate into the subballast layer, forming mud, while coarse eroded particles accumulate at the base, creating low-permeability interlayers. Notably, the geometric conditions alone may not guarantee effective prevention of contact erosion in railway substructures. The hydraulic conditions for contact erosion are more easily achieved under cyclic loading compared to static loading. These distinctive features of contact erosion in railway substructures, different from those observed in hydraulic structures, provide some insights for the development of remediation strategies and improvements in railway substructure design.

Introduction

Internal erosion poses significant hazards to hydraulic structures, especially during flood seasons, and leads to substantial economic losses worldwide[3,29,50,62]. This phenomenon can be classified into four types: erosion in concentrated leaks, backward erosion, contact erosion, and suffusion. Among these, contact erosion, occurring at the interface between two soil layers with significant permeability differences, has been shown to be particularly severe. The migration of fine soil particles through the pores of coarse soil results in severe consequences for dikes and foundations[9,14,20,37,42].

Inevitably, levees or embankment dams consist of layer-distributed soils. Unlike artificial foundations, the overlying soil deposits in natural settings exhibit notable heterogeneity, anisotropy, and stratification [12,58,59]. Additionally, their physical properties, such as density and grain size, cannot be artificially controlled. Interfaces serve as preferential sites for erosion when adjacent soil layers exhibit significant differences in properties, such as gradation and permeability. Such geological conditions are widespread globally. Notably, levees constructed along the Yangtze River in China, the Mississippi River in the United States, and the Kinu River in Japan are all built on grounds characterised by these types of interfaces [41]. In such conditions, contact erosion becomes a potential occurrence as the water level increases. The continuous removal of a significant quantity of fine particles through contact erosion can result in overall deformation of the levee body. Research on contact erosion mechanisms typically employs various laboratory and/or field-testing methods[18,26,36]. Cyril et al. [18] investigated two types of contact erosion and found that vertical

* Corresponding authors at: School of Civil Engineering, Central South University, Changsha 410075, China (S. Zhang).
E-mail addresses: shaoheng.dai@student.uts.edu.au (S. Dai), xuzhen.he@uts.edu.au (X. He), gao-feng@csust.edu.cn (F. Gao), 1575267139@qq.com (W. Zhong), yzheng@whu.edu.cn (Y. Zheng), shengzhang@csu.edu.cn (S. Zhang).

https://doi.org/10.1016/j.trgeo.2025.101499
Received 4 October 2024; Received in revised form 28 November 2024; Accepted 19 January 2025
Available online 22 January 2025

contact erosion and parallel contact erosion often occur simultaneously. Beguin et al. [7] conducted small-scale contact erosion tests and measured the flow characteristics between soil interfaces using particle image velocimetry. With the application of numerical simulation techniques and the development of high-performance computing technology, research based on micromechanics has seen rapid development. Numerical simulation provides a quantitative approach to complement laboratory experiments and offers an in-depth understanding of contact erosion mechanisms from a multiscale perspective [25,26,27,60]. Currently, it is widely recognised that two conditions must be met for contact erosion to occur in hydraulic structures: geometric and hydraulic conditions. The geometric condition requires that the coarse layer and the adjacent layer be geometrically open, allowing fine particles to pass through sufficiently large pores. Extensive research has been conducted on geometric conditions, and reliable standards have been proposed to predict whether particles can pass through coarse material layers with specific grain size distributions[24,33,48,63]. On the other hand, the hydraulic condition depends on factors such as flow velocity and critical hydraulic gradient, which must be sufficient to separate and transport particles [11,15,19,30].

The railway substructure consists of the roadbed (including ballast and/or subballast) and subgrade, as depicted in Fig. 1. It should be noted that each layer in the railway substructure serves different functions, closely related to the grain size distribution of the materials used. The subgrade is typically constructed using densely compacted sandy soils, while the roadbed is comprised of elastic gravel with high-strength characteristics. The railway substructure represents a typical stratified structure, with significant differences in permeability between the soil layers, making it susceptible to contact erosion. However, current studies rarely discuss contact erosion occurring in the railway substructure. This is mainly because the critical hydraulic gradient or flow velocity required for contact erosion to occur is typically high. Unlike hydraulic structures such as dams, railway substructures generally have favourable hydrogeological conditions with well-drained roadbeds, making it challenging to reach the critical hydraulic conditions for contact erosion. As a result, the filtration criteria (geometric conditions) for railway substructures are usually not required to be overly strict or high-quality.

However, in the current era of global climate change, railway substructures are increasingly prone to high water content induced by extreme weather events such as heavy rainfall, storm surges, ocean waves, and flash floods [21,49,61]. Regions with extensive development of high-speed railways, such as southeastern China, frequently experience heavy rainfall. Excessive rainwater infiltration into the railway subgrade leads to the generation of large amounts of slurry under the repeated action of train loading on ballastless tracks, resulting in a significant deterioration in track performance[8,43]. Additionally, high groundwater levels pose challenges to the performance of railway substructures. Australia's heavy-duty railway system, one of the world's largest freight train networks, is particularly affected due to its proximity to the ocean, resulting in high groundwater levels that keep the railway subgrade saturated for extended periods, intensifying the impact [46]. Mud pumping has been observed at over 300 locations along the coastal line in New South Wales[1,45]. Given the frequent occurrence of heavy rainfall and fluctuations in the groundwater table during the service life of the railway substructure, the likelihood of contact erosion increases. This erosion mechanism, involving long-term damage, poses significant challenges to passenger comfort and operational safety. Therefore, studying the mechanisms of contact erosion in railway substructures and deepening our understanding of the migration of fine particles under the combined action of stress and hydraulic conditions is crucial.

Historically, the development of erosion testing apparatus has primarily focused on studying filter criteria and contact erosion mechanisms in embankments and dikes. There has been limited emphasis on specifically targeting erosion in railway substructures. Consequently, an appropriate experimental apparatus is designed to simulate contact erosion in the laboratory setting. This apparatus serves the purpose of investigating the fundamental phenomena involved, quantifying the migration processes of fine particles within the railway substructure, and identifying the parameters controlling erosion. The structure of this paper is as follows: Section 2 introduces the setup of the experimental apparatus. Section 3 provides the migration patterns of particles during contact erosion. Section 4 discusses the reasons for the erosion damage to railway substructures. Finally, Section 5 highlights the limitations of the study, while Section 6 summarises the key findings.

Contact erosion test

Apparatus

An apparatus is designed to conduct erosion tests, simulating conditions relevant to railway substructures and replicating contact erosion. The design, depicted in Fig. 2, is inspired by various devices developed for testing embankment dam filters [11,19,36,38,41]. Necessary modifications have been made to the erosion test apparatus to accurately simulate contact erosion in railway substructure. The newly developed apparatus primarily consists of a substructure model base, a water supply system, a data acquisition system, and an axial loading system.

The water supply system simulates the hydraulic conditions experienced in railway substructure. One of the main objectives of this study is to replicate contact erosion under the influence of groundwater and train loads. To achieve this, water is supplied from the bottom of the sample via a water tank, simulating groundwater levels typical in areas with high water tables or during rainfall. To minimise the effect of water flow on the water tank's head, a buffer tank is also included. Additionally, a buffer zone is added at the base of the substructure model to ensure a uniform water flow into the specimen, reducing the direct impact on the sample itself.

The data acquisition system includes pore water pressure sensors, a turbidity meter, and data acquisition software for real-time monitoring and data processing. Turbidity measurements estimate the concentration of suspended particles within the substructure, providing an indication of the extent to which fine particles have been eroded and

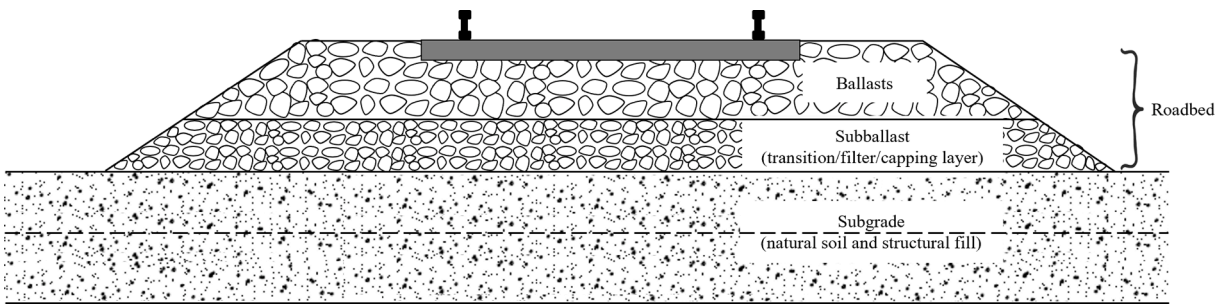

Fig. 1. Typical diagram of railway substructure.

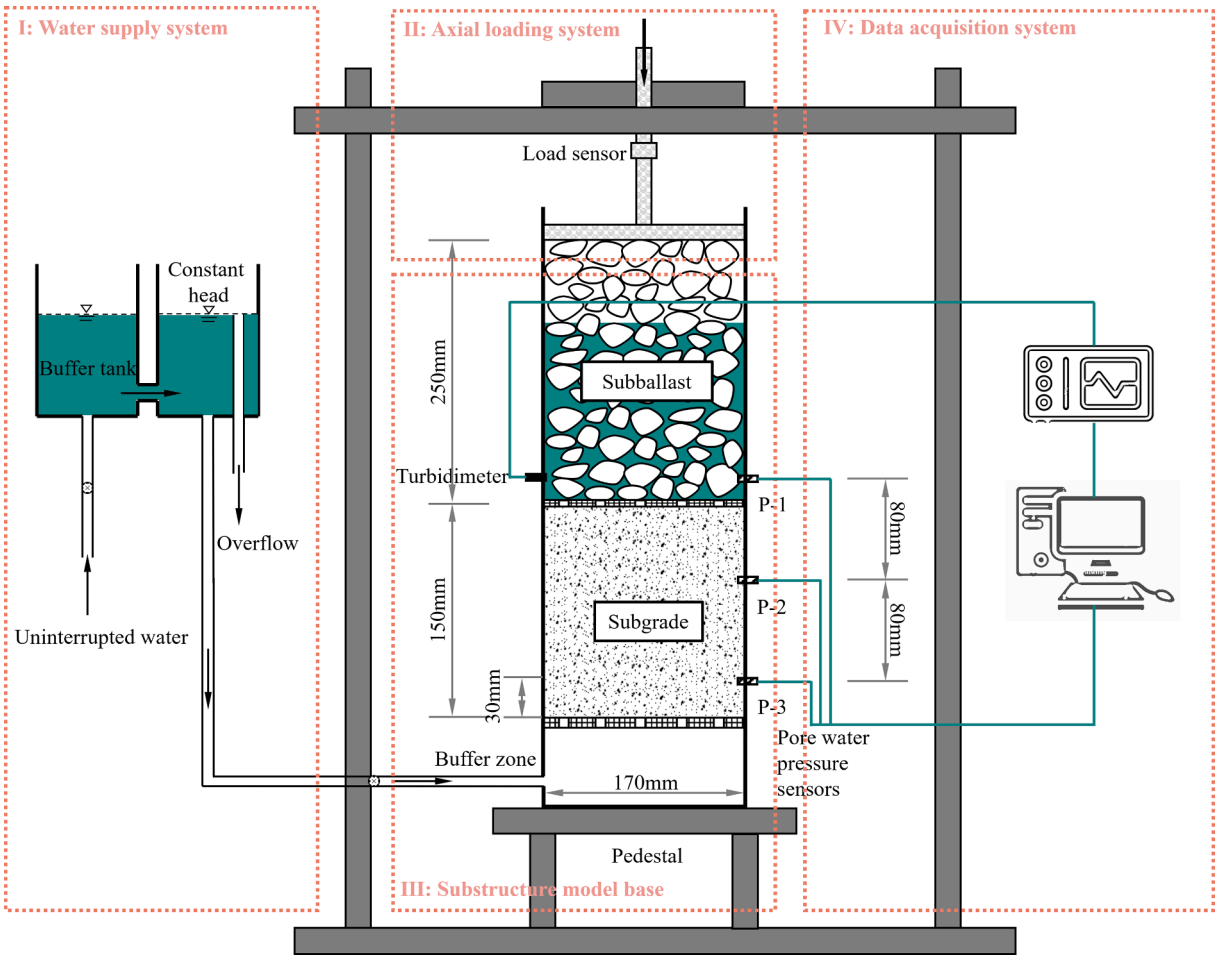

Fig. 2. General layout of the testing apparatus.

transported by the flow. Three pressure transducers, namely P-1, P-2, and P-3, are installed on the wall of permeameter at depths of 30 mm, 110 mm, and 190 mm from the bottom of specimen, respectively. Prior to preparing the specimen, these installed pressure sensors are soaked in de-aired water for 24 h to ensure accurate measurements.

In accordance with ASTM D2434-68 [4], the permeameter used in the experimental setup is designed cylindrically to eliminate unnecessary preferential flow paths at corners. The permeameter has a minimum diameter of approximately 8 times the maximum particle size to ensure the accuracy of tests. Therefore, the base of substructure model is constructed using a 10 mm thick clear acrylic cylinder with an internal diameter of 170 mm and a height of 500 mm.

The axial loading system replicates the stress conditions of railway substructures by applying static or cyclic loads to the top of specimen, thereby simulating realistic loading scenarios. Unlike traditional contact erosion equipment, this device incorporates an axial loading system, which uniquely allows for the study of contact erosion between subgrade and subballast under cyclic loading and specific hydraulic conditions. Further details of the device are provided in the following sections.

Methodology

The subgrade material is carefully packed into three layers, each with a thickness of 50 mm, employing the Layer Compaction Method to ensure proper compaction. The relative density of the subgrade material is set at 90 % to achieve the desired engineering properties. The coarse aggregate (subballast) layer, with a thickness of 250 mm, is compacted to a degree of compaction of 95 %. To prevent subballast intrusion into the subgrade layer under cyclic loading[22,23], a wire mesh with a 4 mm pore size is placed between the subballast and subgrade. This metal wire mesh allows the subgrade material to flow with water while mitigating the intrusion of subballast from the upper layer. After filling the specimen, static loading is applied to the top of specimen. Subsequently, the height of water tank is gradually raised to reach the designed water level. The rate of water level rise is carefully chosen to be small enough to avoid disturbing the soil structure during saturation. Sufficient time is provided for the railway substructure to reach saturation.

Upon reaching the desired saturation period, the axial loading device is activated, and cyclic loading is applied to the specimen for about 10 h. During this period, the water level in the tank remains constant. The cyclic loading in this study is characterised by specific strength parameters, with average stress and amplitude of 28 kPa and 6 kPa, respectively, at a frequency of 10 Hz. It is worth noting that these loading conditions closely resemble the dynamic stress generated by the CRH-380A high-speed train on the Wuhan-Guangzhou line, with speeds ranging from approximately 250 to 350 km/h and an axle load of 15–20 tonnes[19,63]. Following the completion of the cyclic loading, the specimen is divided into three layers: the subgrade layer, the interface layer, and the subballast layer. The particle size distribution (PSD) of each layer is determined by re-sieving, providing data for further analysis.

Materials

The testing materials used in the study comprise of gravel and sandy soil, representing the subballast and subgrade soil, respectively. Prior to testing, the gravel undergoes a cleaning process to remove fouling from

the particle surfaces. The sandy soil, serving as the subgrade soil, is collected from the Xiangjiang River Basin in Changsha, China. This sandy soil is commonly used in the construction of embankments for the Wuhan-Guangzhou high-speed railway. Due to its ideal properties, such as high permeability and low compressibility, sandy soil is widely utilised in engineering applications. However, natural sandy soil typically contains a certain amount of fines (particles smaller than 0.075 mm), which are crucial in the erosion process and are most susceptible to loss during erosion. Therefore, the fines content in soil significantly influences erosion behaviour. In China, the "Code for Design on Subgrade of Railway (TB 10001–2005)"[16] imposes specific limits on the fines content of subgrade soils. In this study, the sandy soil is dried and processed to separate particles smaller than 0.075 mm as fines, while particles larger than 0.075 mm are categorised as sand grains. To investigate the impact of fines content on erosion, four different binary mixtures are prepared, with fines contents of 0 %, 8 %, 16 %, and 24 % by mass. It is worth emphasising that the subgrade soil used in this study complies with the requirements specified in the "Code for Design on Subgrade of Railway (TB 10001–2005)"[16]. The particle size distribution curves of the subballast and subgrade materials employed in this study are similar to those recommended for railway substructure soils in the Chinese standard "Code for Sub-ballast in Gravel Roadbeds of Railways (TB/T 2897–1998)"[17]. The particle size distribution and physical properties of the materials are presented in Fig. 3 and Table 1, respectively.

An adequate hydraulic gradient is a key index of whether soil erosion can occur. In this study, the pressure heads at the bottom of subgrade soil are fixed at 20 cm, 30 cm, and 40 cm, respectively, to examine the influence of groundwater levels during rainfall or in water-rich regions on contact erosion. The use of dimensionless parameters can make graphs and tables more concise and results more universally applicable. Therefore, the pressure head is normalised based on the thickness of the subgrade soil (15 cm). Twelve tests are conducted under varying conditions characterised by two parameters: initial fines content, and pressure head. These test cases aim to explore the influence of these factors on contact erosion. Table 1 summarises the experimental conditions and parameters considered in this study.

Experimental results

Table 2 presents the experimental results obtained from the study. It is observed that when the pressure head is 1.33, the combined effect of cyclic loading and pressure head does not induce the loss of fine particles. Consequently, no contact erosion is observed in any specimens with a pressure head of 1. 33. The results indicate the existence of a critical pressure head, beyond which contact erosion occurs in the specimen. Specifically, under cyclic loading, fine particles begin to jump

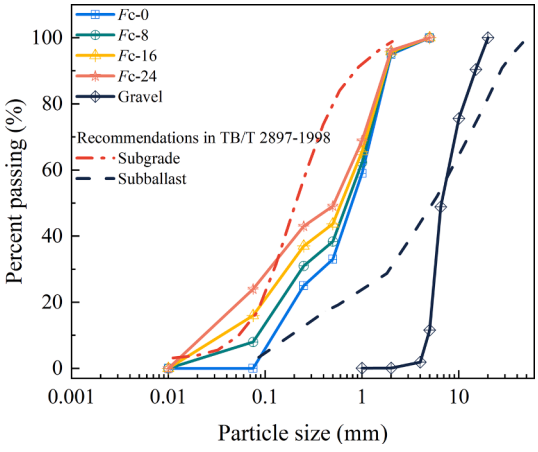

Fig. 3. Particle size distribution of materials.

Table 1
Basic physical properties of the specimen.

Sample identifier	Maximum dry density ρ_{dmax}/(g/cm^3)	Minimum dry density ρ_{dmin}/(g/cm^3)	Coefficient of curvature (C_c)	Coefficient of uniformity (C_u)	Pressure head
Fc-0	1.94	1.53	1.11	7.09	1.33,
Fc-8	1.96	1.55	0.68	10.56	2.00,
Fc-16	1.98	1.59	0.83	17.24	2.67
Fc-24	2.07	1.67	0.59	20.93	

Table 2
Summary of experimental results.

Specimen	Pressure head		
	1.33	2.00	2.67
Fc-0	N	N	Y
Fc-8	N	Y	Y
Fc-16	N	Y	Y
Fc-24	N	Y	Y

Note: "N" means no erosion; "Y" means erosion.

dramatically, migrating through the localised pore water flow. These suspended particles move upward into the subballast layer, indicating the occurrence of contact erosion. The particle migration process can be divided into two stages. Initially, fine particles detach from the soil skeleton, no longer transmitting intergranular stresses. Subsequently, under the combined influence of pressure head and cyclic loading, these fine particles infiltrate the subballast layer. Consequently, the turbidity of the subballast layer rapidly increases.

Evolution of turbidity in subballast layer

To quantitatively characterise the degree of contamination in railway substructures, fouled subballast parameters such as Void Contaminant Index (VCI) [51], Percentage Void Contamination (PVC) [10], and mud turbidity [52,53] have been proposed. In this study, the mud turbidity is used to represent the degree of contamination during testing. Turbidity is defined as the mass of soil particles per unit volume of slurry and is measured using the turbidimeter [63]. The calculation is expressed as:

$$Tu = \frac{m_{soil}}{V} \tag{1}$$

where Tu represents turbidity (g/L), m_{soil} is the mass of soil particles in the slurry (g), and V is the water volume in the slurry (L).

During the experiments, the mud turbidity of subballast layer is measured every half hour, with the evolution of turbidity illustrated in Fig. 4. It should be noted that in experiments with lower pressure heads and fines content, no contact erosion occurred. Therefore, the results from these experiments are not presented. Fig. 4 depicts that during the initial stages of cyclic loading, the turbidity of the subballast layer rapidly increases, indicating an influx of soil particles. Under dynamic hydraulic action, fine particles diffuse into the pore water, forming a suspension and migrating within the pores. An increase in pressure head leads to a significant increase in turbidity. For instance, at a pressure head of 2.67, the turbidity of *Fc*-24 is approximately twice that at a pressure head of 2. Similarly, higher fines content corresponds to higher turbidity values. For example, at a pressure head of 2.67, the turbidity of *Fc*-24 is about 3.5 times that of *Fc*-0. As cyclic loading progresses, the rate of particle detachment decreases, and the turbidity of subballast layer stabilises, reaching a dynamic steady state with slight fluctuations. The time required to achieve this steady state increases with higher fines content. The average turbidity value over the final 120 min of loading is

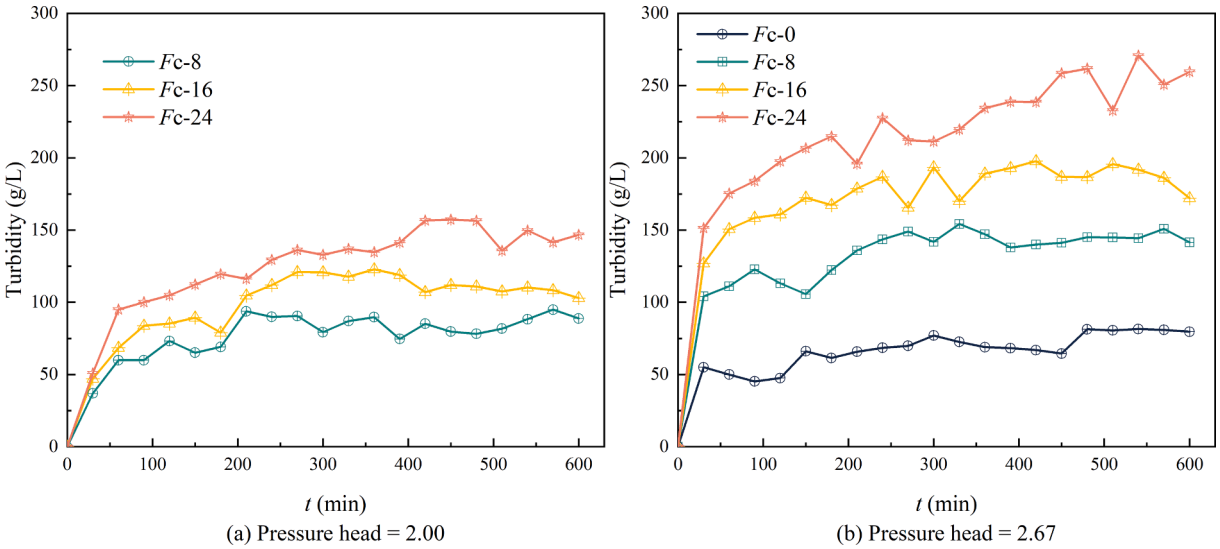

Fig. 4. Evolution of mud turbidity in the subballast layer.

used to represent this steady state. Fig. 5 describes the relationship between steady-state turbidity and fines content at different pressure heads, showing a linear increase in steady-state turbidity with higher fines content at the same pressure head. This increase in turbidity is attributed to the instability of fines under dynamic hydraulic conditions, leading to greater migration of fines into the subballast layer. Additionally, the effect of fines content on turbidity is more pronounced at higher pressure heads. For example, at a pressure head of 2.67, the rate of turbidity increase with fines content is approximately twice that observed at a pressure head of 2.

After stopping cyclic loading, some soil particles settle to the bottom due to gravity, while others deposit and adhere to the surface of the subballast. Fig. 5 also shows turbidity measurements of the subballast layer taken 12 h after the cessation of cyclic loading. It is evident that turbidity significantly decreases after loading stops and increases linearly with higher fines content. The deposition characteristics within the subballast layer are closely related to the slurry composition and pore structure of the gravel layer [6]. It is important to note that the dispersion of fine particles into the subballast layer contributes to subballast fouling, which can impair track performance. Consequently, track maintenance or upgrading may be necessary to ensure reliable and safe operations.

Particle loss from the sandy soil layer

The PSD of the sandy soil is affected by the migration of fine particles into subballast layer. Following the test, the PSDs in the top, middle, and bottom layers are determined through sieving. Fig. 6 illustrates the PSD curves for *Fc*-16 (with a pressure head of 2.67), showing noticeable differences between the pre- and post-test. Since coarse particles form a soil skeleton that is difficult to move, their mass changes only slightly. The variations in PSD primarily occur in the fine-grain fraction, attributed to the loss of fine particles due to seepage effects. Similar changes in PSD are observed in the other test groups as well. Additionally, sieving the subballast after the test reveals that the lost particles have a maximum diameter of 1–2 mm. These research findings suggest that the migration of fine particles from the subgrade soil to the subballast layer, as evidenced by changes in the PSDs, can change the soil mixture composition. This may potentially impact track performance and maintenance.

Based on the changes observed in the cumulative mass grading curve before and after the test, Kenney and Lau [39] introduced the Particle Loss Index, a widely used metric for characterising particle loss. It is assumed that the coarse skeleton remains unchanged while fine particles are lost. Consequently, the mass of coarse particle group remains constant, but its proportion increases. The cumulative mass grading curves

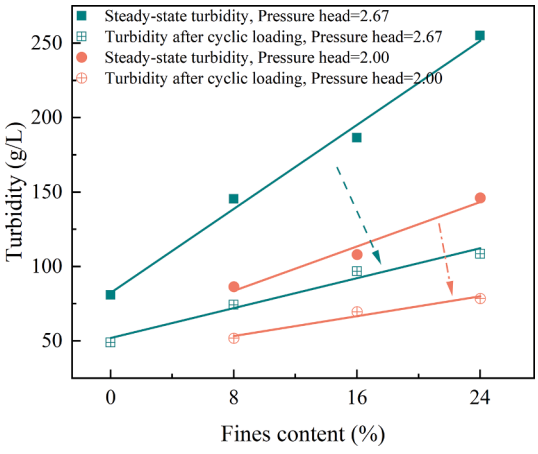

Fig. 5. Variation of turbidity after cyclic loading stops.

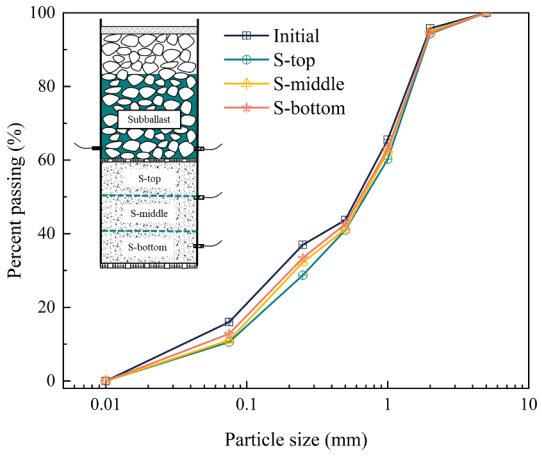

Fig. 6. Variations in PSD for *Fc*-16 at a pressure head of 2.67 before and after testing.

before and after the test are same within the particle size range where no loss occurs, but they differ within the particle size range where loss happens. As illustrated in Fig. 7, the degree of particle loss can be calculated by constructing an extended gradation. In this study, the Particle Loss Index is employed to assess the degree of particle loss in the top, middle and bottom layers of sandy soil under cyclic loading.

Fig. 8 illustrates the distribution of the Particle Loss Index along the depth of specimen. It is noteworthy that Particle Loss Index reflects the overall degree of loss, considering not only the quantity of particles lost within a specific layer but also the impact of particle loss from lower soil layers. The Particle Loss Index incorporates the effects of clogging and filling when particles lost from lower layers traverse the examined layer, occasionally resulting in negative values. As depicted in Fig. 8, the Particle Loss Index is highest in the top layer of sandy soil, primarily due to the shorter migration path of fine particles. However, the middle layer exhibits a more complex pattern, with some specimens showing negative values. This phenomenon can be attributed to the extended potential migration distance of fine particles, which increases the likelihood of encountering small pores that impede further migration and cause clogging. Consequently, the mass of fine particles lost from this layer may be less than that of fine particles migrating into this layer from lower layers. In contrast, negative values are not observed in the bottom layer, as no particles migrate to this layer.

The relationship between pressure head and particle loss is evident: as the pressure head increases, the seepage force under cyclic loading becomes stronger, leading to greater particle loss. Additionally, Fig. 8 demonstrates that an increase in fines content also results in increased particle loss. Particle loss in the sandy soil layer is essentially a suffusion process, prompting an evaluation of the soil's vulnerability using four established methods [35,39,40,55]. The evaluation results are presented in Table 3. As fines content increases, the stability of the sandy soil decreases. Moreover, since particles involved in internal erosion are typically small, higher fines content leads to a greater number of mobile particles. This assessment is consistent with the experimental results: for example, Specimen *Fc*-0, which shows potential stability against suffusion, exhibits lower turbidity in the subballast layer and less particle loss in the sandy soil layer. Conversely, Specimen *Fc*-24 demonstrates potential instability, leading to significant erosion loss.

The mechanism of contact erosion in railway substructures

The phenomenon of particle migration in railway substructures is inherently complex, posing significant challenges in understanding its underlying mechanisms. This research aims to illustrate the behaviour of particle migration within railway substructures, with a specific focus on the example of *Fc*-16. Our analysis centres on the concept of contact erosion, providing some insights into this intricate process. By exploring the mechanisms of particle migration, we hope to deepen our understanding of its behaviour and implications in railway substructures.

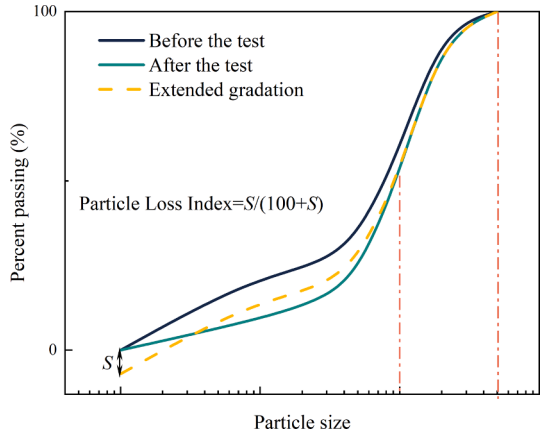

Fig. 7. Diagram of the Particle Loss Index calculation.

Evolution of pore water pressure

Before the onset of cyclic loading, a static load of 28 kPa is applied to the top of the specimen. Notably, experimental observations during this stage reveal that the slurry turbidity remains at 0 within the range of pressure head imposed by the test. This indicates that the applied pressure head is insufficient to trigger fine particle migration. However, once cyclic loading begins, erosion and migration of fine particles within the sandy soil layer occur, leading to a rapid increase in turbidity within the subballast layer. This phenomenon demonstrates that cyclic loading introduces an additional "driving force" that facilitates fine particle migration. It's noteworthy that the development of pore water pressure is closely linked with particle migration, as emphasised in previous research [2,19,32,44]. Therefore, variations in pore water pressure in the subballast layer and sandy soil layer will be analysed separately.

The pore water pressure curves for the subballast layer during contact erosion are presented in Fig. 9. The results indicate that under static loading, pore water pressure remains constant, with higher pressure heads corresponding to higher pore water pressures. However, under cyclic loading, significant fluctuations in pore water pressure are observed. As the pressure head increases, the amplitude of pore water pressure fluctuations in the subballast layer also rises significantly. The oscillations in pore water pressure at the sandy soil-subballast interface generate oscillatory seepage forces, disrupting the contact between particles. This increase in pressure head not only enhances the permeation force acting on the particles but also disrupts the overall structure of the sample, making the particles more susceptible to migration.

Fig. 10 illustrates the variation of pore water pressure in the sandy soil layer. The application of cyclic loading induces a rapid increase in pore water pressure, with the magnitude of sudden increments growing as the pressure head increases. Meanwhile, turbidity in the subballast layer exhibits a higher growth rate. Compared to the trend in pore water pressure in the subballast layer, the changes in pore water pressure within the sandy soil layer are more complex. With continued cyclic loading, pore water pressure at P-3 gradually dissipates, while at P-2, it dissipates faster and subsequently undergoes oscillations. This observation is consistent with the pore water pressure development reported by Ueng et al. [54]. The oscillations in pore water pressure are attributed to significant particle losses occurring at P-2, resulting in changes in the soil's spatial structure and an overall increase in porosity. Under the influence of cyclic loading, pore water pressure in the sandy soil layer with increased porosity follows a trend similar to that in the subballast layer, accompanied by minor oscillations. In summary, cyclic loading leads to excessive pore water pressure in the sandy soil, with the magnitude of pressure increments increasing with the rise in pressure head. The dissipation of pore water pressure in the upper portion of the sandy soil is relatively rapid, followed by oscillations.

Evolution of the grade distribution at the interface layer

To initiate contact erosion, a geometric condition must be met: the constrictions, which are the smallest sections of the pore network in the coarse soil, must be sufficiently large for the eroded particles to pass through[7]. The presence of a coarse layer acts as a filter that influences the migration behaviour of soil particles. Observations from the tests, illustrated in Fig. 11, show fine eroded particles entering the subballast layer and forming a slurry material. Conversely, coarser eroded particles tend to accumulate at the base of the subballast, creating a secondary backfilter layer that hinders further particle migration. These findings are consistent with the results reported by Duong et al. [22,23], which also highlight the presence of such low-permeability interlayers.

Fig. 12 displays the PSD of interface layer after testing. Compared to the initial PSD curve, the post-test curves show an upward shift,

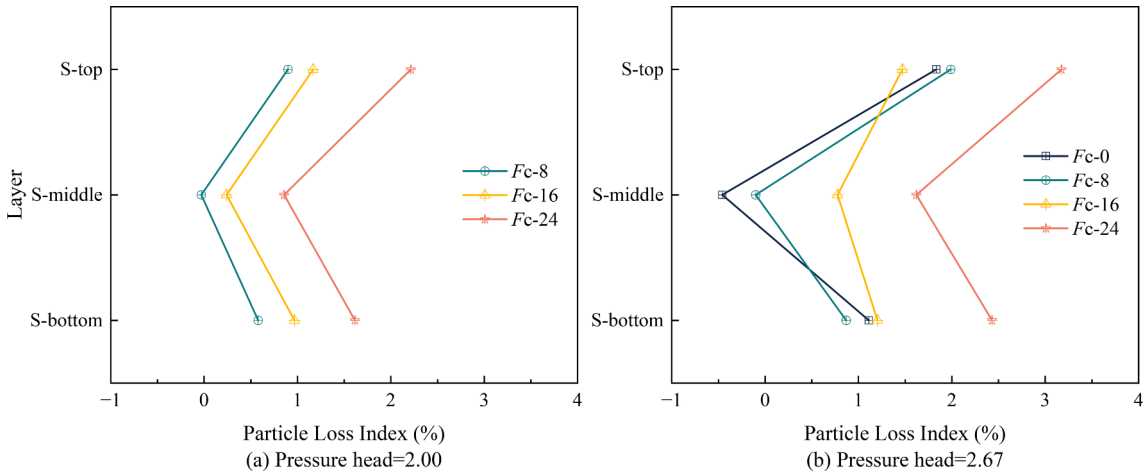

Fig. 8. Distribution of Particle Loss Index across different layers of sandy soil.

Table 3
Assessment of internal stability of sandy soil.

Methods used for assessing internal stability		Internal stability			
Criteria	The sandy soil is Internally Stable if	*Fc*-0	*Fc*-8	*Fc*-16	*Fc*-24
US Army Crops Engineering Engineers (1953)	$C_u < 20$	S	S	S	U
Istomina [35]	$C_u \leq 20$	S	S	S	U
Kezdi [40]	$D_{15c}/d_{85f} \leq 4$	S	S	S	S
Kenney and Lau [39]	$(H/F)_{min} >= 1$ $(0 < F < 0.2)$	S	S	U	U

Note: C_u = coefficient of uniformity; soil could be divided into a coarse fraction (c) and a fines fraction (f). D_{15c} = the grain size finer than which 15 % of the coarse fraction is retained; d_{85f} = the grain size finer than which 85 % of the fines fraction is retained; $h_1 = d_{90}/d_{60}$; $h_2 = d_{90}/d_{15}$; "U" denotes unstable; "S" denotes stable.

primarily due to the blockage of subballast pores by soil particles. Typically, the amount of eroded soil increases with prolonged soil–water contact time. However, the tests reveal that the development of contact erosion is not continuously noticeable, and turbidity eventually stabilises at a relatively steady-state value. This stabilisation is largely due to the formation of a low-permeability interlayer at the subballast-sand interface, which results in more tortuous migration channels [64]and slows the contact erosion process in railway substructures. The Terzaghi retention criterion[56], originally developed for cohesive uniform base soil and filter materials, is widely used to assess filtration performance. The retention ratio (D_{15}/d_{85}) is defined as the ratio of D_{15} (size at which 15 % by mass of particles are finer) for the filter material to d_{85} (size at which 85 % by mass of particles are finer) for the base soil. According to the Terzaghi criterion, a retention ratio below 5 is necessary to prevent significant particle loss. Fig. 13 presents an assessment of the filtration performance of the interface layer based on this criterion. It can be observed that the subballast layer exhibits effective filtration. As the fines content in the sandy soil increases, a lower retention ratio (D_{15}/d_{85}) indicates a greater loss of particles. The accumulation of coarser eroded particles changes the grading distribution at the bottom of subballast layer. For instance, at pressure heads of 2 and 2.67, the retention rates of the interlayer in *Fc*-16 decrease from 3.86 to 1.09 and 0.74, respectively. Contact erosion in railway substructures leads to the formation of a secondary backfilter layer, and the presence of a low-permeability interlayer impedes particle migration, thereby enhancing the effectiveness of the subballast layer as a filter. However, it should be noted that the permeability of subballast is closely related to the PSD. While the formation of a secondary backfilter layer can improve filtration efficiency, it significantly reduces permeability and drainage properties, which is considered one of the main causes of railway failures, such as mud pumping.

Discussion

A key characteristic of railway substructure is the interaction between the fine layer (sandy soil) and the coarser layer (subballast), which is particularly susceptible to contact erosion. These interfaces, with their significant permeability differences, serve as preferential sites for erosion. Contact erosion primarily involves the migration of particles. If the contractions connecting the pores of coarse soil are too narrow, fine particles are unable to pass through. In this case, the coarse soil

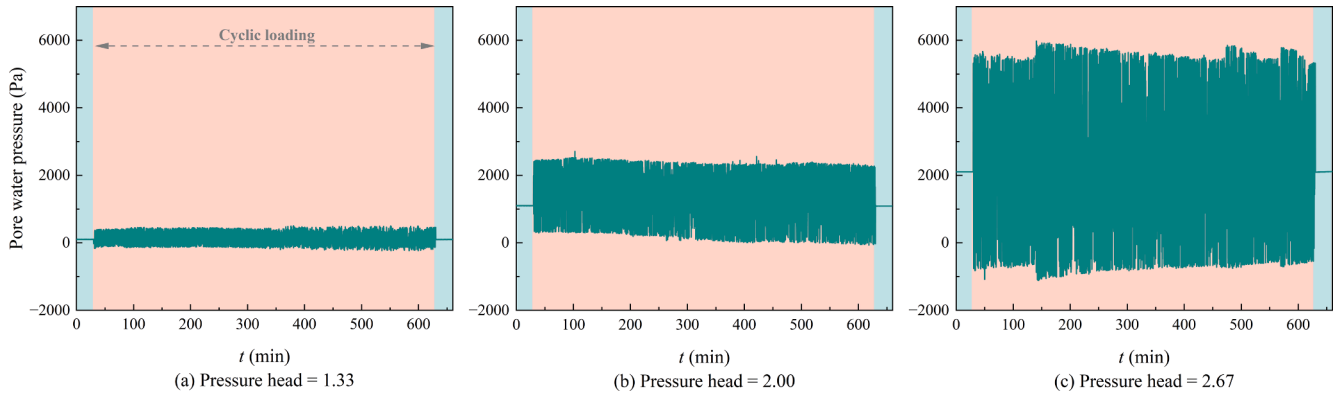

Fig. 9. Variations of pore water pressure in the subballast layer.

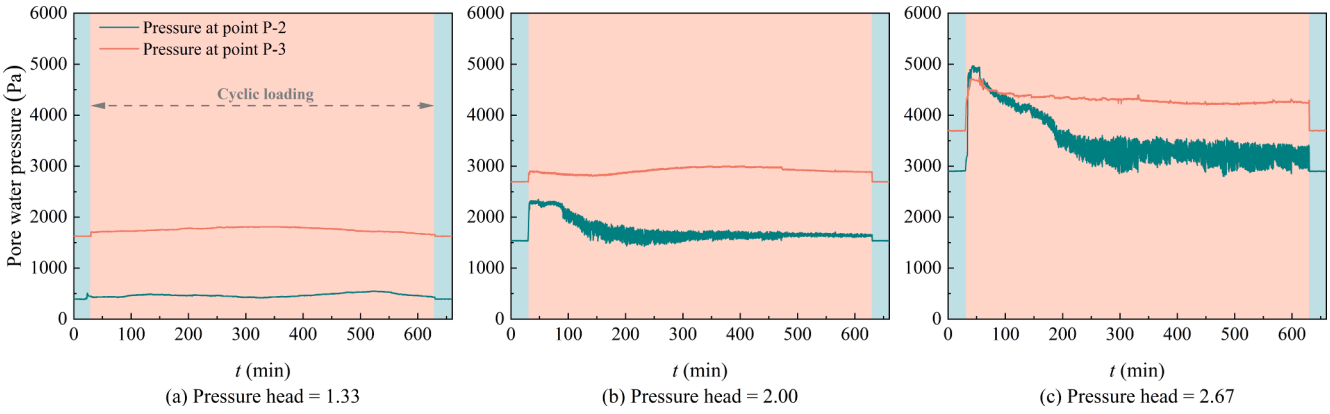

Fig. 10. Variations of pore water pressure in the sandy soil layer.

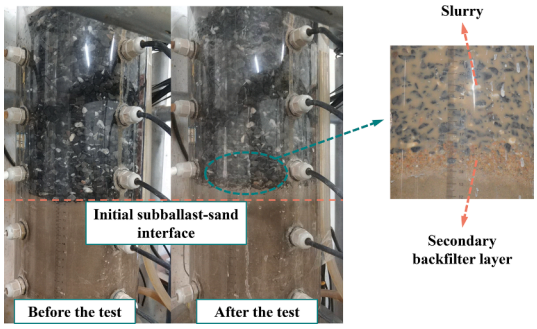

Fig. 11. Observations before and after the test.

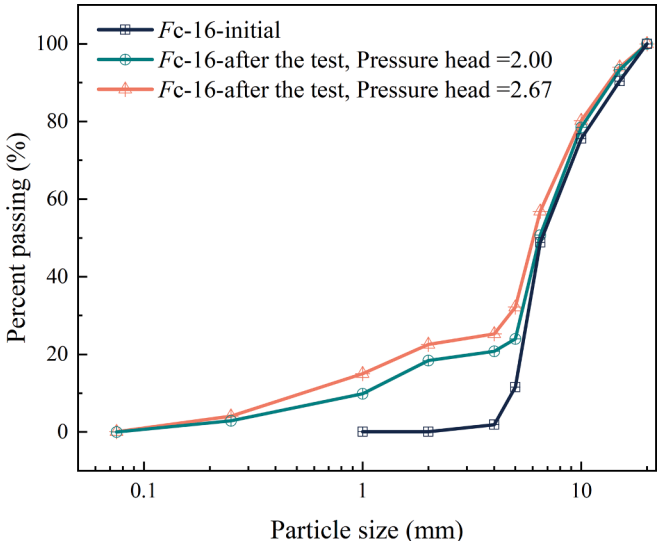

Fig. 12. Changes of PSD in the interface layer of *Fc*-16 before and after testing.

is considered "geometrically closed." However, if the contractions are large enough to allow particle passage, a hydraulic criterion must be met by the flow to initiate erosion and particle migration.

The geometric condition

The combination of coarse soil and base soil is generally considered suboptimal for filtration design and is typically discouraged. However, some railway substructures may feature these arrangements. As depicted in Fig. 1, railway substructures consist of a roadbed and subgrade, with the main function of the roadbed being to provide sufficient

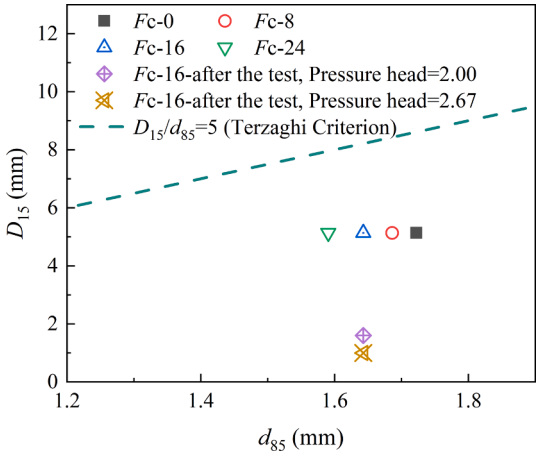

Fig. 13. Filtration analysis of the specimen.

strength for the superstructure. Historically, ballast selection primarily focused on strength, with little emphasis on filtration. For example, in France, conventional rail lines were constructed by directly installing ballast onto the subgrade without a separation layer, accounting for 94 % of the entire railway network [23]. Over time, with the continuous increase in train speeds, erosion-related issues in the substructure have become more prevalent. To address these problems, the inclusion of a subballast layer has been implemented in recent years to mitigate erosion between the upper ballast layer and the lower subgrade. Filter criteria [34], developed by the U.S. Army Engineer Waterways Experiment Station [56] and the U.S. Bureau of Reclamation [57], have been applied in these cases. Two separation gradation criteria are commonly used:

$$D_{15} \leq 5d_{85} \tag{2}$$

$$D_{50} \leq 25d_{50} \tag{3}$$

where D_n represents the filter grain size at which n percent of the total weight of the filter material passes through, and d_n represents the base particle size at which n percent of the total weight of the base material passes through.

According to the research by Indraratna et al. [34], the criterion described in Equation (2) ensures that the coarsest end of the protected soil (d_{85}) is blocked by the finest end of the filter (D_{15}). This configuration effectively prevents particle migration and ensures that the filter retains particles within the protected soil. The criterion outlined in Equation (3) aims to avoid the use of gap-graded filters by promoting the filter grading closely paralleling the grading of the protected soil. By

closely matching the particle sizes between the filter and the protected soil, this criterion enhances the effectiveness of the filtration system. It reduces the likelihood of particle migration and ensures that the filter performs its intended function of retaining particles. In summary, both criteria are critical in the design of effective filtration systems for railway substructures. While Equation (2) focuses on preventing particle migration by blocking the coarsest particles, Equation (3) emphasises the importance of a well-graded filter that complements the protected soil, thereby improving filtration performance and reducing the likelihood of particle migration.

Fig. 14 presents the selected coarse aggregate material used in this study, illustrating its compliance with established filter criteria. However, despite the use of appropriate coarse aggregate materials for the subballast, effective control of erosion in the base soil (sandy soil) has not been fully achieved. The figure also references various studies [5,8,13,23,28,47,53,52,63] that highlight ongoing erosion issues in railway substructures. These studies indicate that some materials used in railway construction do not consistently meet filter criteria. Although current practices prioritise meeting the filter criteria for new railway substructures, there are situations where in-situ materials must be used, and their filtration effectiveness may not be ideal. Additionally, older railway lines often lacked consideration of filter criteria during their construction, leaving their long-term performance uncertain. Even when materials comply with filtration standards, as depicted in Fig. 14, failures in filtration systems can still occur. The Terzaghi criteria, widely regarded as reliable in dam filtration design, may not fully address the unique challenges posed by cyclic train loads in railway substructures. Dai et al. [19] and Trani and Indraratna [52,53] confirm that cyclic loads significantly impact erosion stability, supporting this view. In conclusion, while advancements have been made in meeting filter criteria for new railway constructions, there remains a need for greater attention to the use of in-situ materials and the performance of older railway lines. Additionally, the impact of train loads on erosion stability presents unique challenges that require careful consideration in the design and maintenance of railway substructures.

The hydraulic condition

Even if the filter criterion is not met, this does not necessarily guarantee the occurrence of contact erosion. Hydraulic conditions must be satisfied for water flow to induce erosion. Typically, contact erosion requires relatively high critical hydraulic gradients. Railway substructures, with good drainage properties, generally do not reach the hydraulic conditions required for contact erosion. However, some specific circumstances such as prolonged flooding or elevated groundwater levels can lead to saturation of materials within railway substructures[1,8,19,31,43,45]. Under these saturated conditions, fine particles may detach and migrate through the pores of coarse soil layer.

In this study, it was observed that under static loading and within the range of applied pressure head, fine particles did not migrate. However, the introduction of cyclic loading while maintaining a constant pressure head led to a significant increase in turbidity in the subballast layer. This indicates that cyclic loading serves as an additional "driving force" for particle migration. Fig. 15 illustrates the pore water pressure of specimen *Fc*-16 at a pressure head of 2.67. During static loading, the pore water pressure at point P-1 is approximately 2.2 kPa. However, with the introduction of cyclic loading, the pore water pressure fluctuates with an amplitude of approximately 3 kPa, including instances of negative pore water pressure. As shown in Fig. 9, an increase in pressure head results in a corresponding increase in the amplitude of pore water pressure fluctuations at P-1.

To evaluate the hydraulic gradient between different layers of the specimen, the measured pore water pressure is converted into pressure head, denoted as H, using the equation $H = u/(\gamma_w)$, where u represents the pore water pressure, and γ_w is the unit weight of water. When the pore water pressures at the locations of P-1, P-2, and P-3 differ, the hydraulic gradient, denoted as i, in each zone is defined as follows [19,54]:

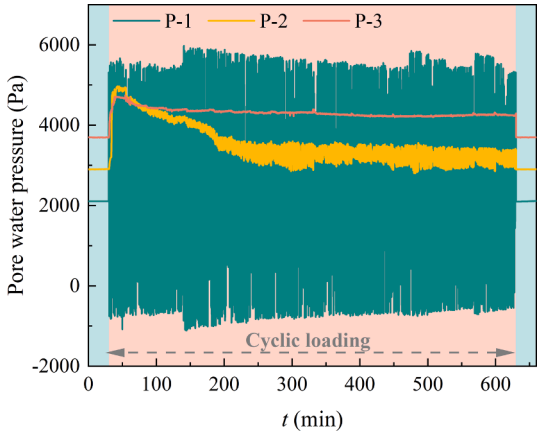

Fig. 15. Time curve of pore water pressure of specimen *Fc*-16.

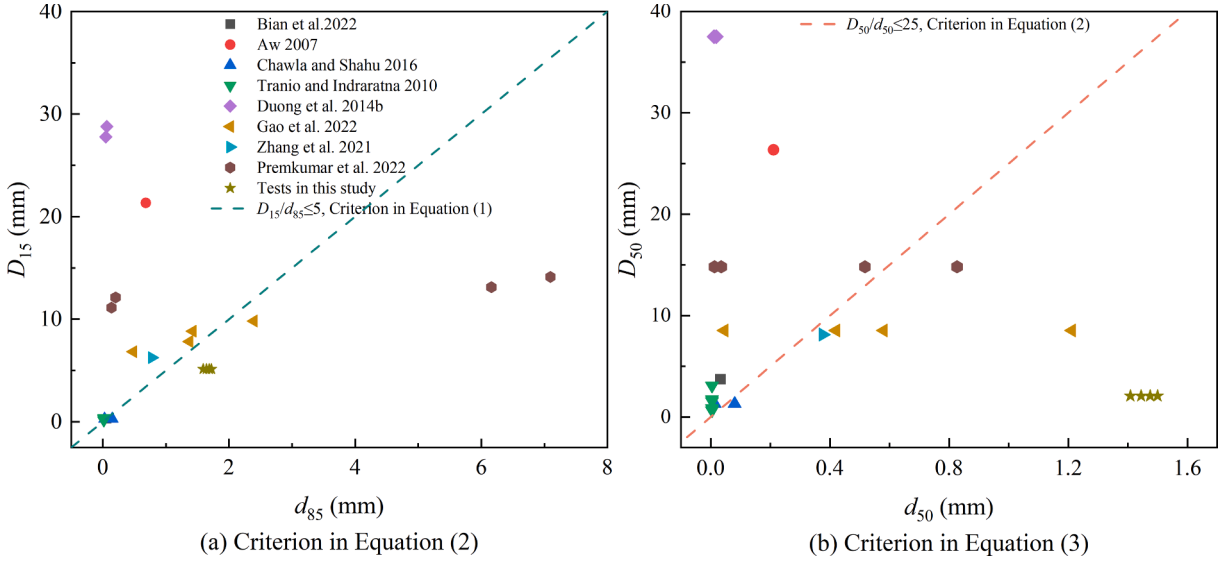

Fig. 14. Failure cases of railway substructures.

$$i_{ij} = \frac{(H_i + Z_i) - (H_j + Z_j)}{L} \quad (4)$$

Here, i_{ij} represents the hydraulic gradient between zone P-*i* and P-*j*, H_i and H_j represent the pressure head at pressure senior P-*i* and P-*j*, respectively, while Z_i and Z_j represent the elevation head at pressure senior P-*i* and P-*j*; and L represents the thickness between the P-*i* and P-*j*. Therefore i_{12} indicates the local hydraulic gradient at the subballast-sandy soil interface, while i_{23} represents the local hydraulic gradient within the sandy soil.

The statistical results of hydraulic gradient i_{ij} between layers are presented in Fig. 16. Under static loading, the hydraulic gradients generated are insufficient to drive the migration of fine particles, resulting in zero turbidity in the subballast layer. However, when cyclic loading is applied, significant fluctuations in pore water pressure are observed, leading to large transient hydraulic gradients at the interfaces and within the sandy soil layer. These transient fluctuations, caused by the dynamic vibrations of the soil under cyclic loading, induce interactions between soil particles and pore water. This interaction generates pulsed dynamic water pressures, which in turn lead to oscillations in the local hydraulic gradient within the sample layers. At certain moments, these transient hydraulic gradients reach the critical threshold for initiating contact erosion, which triggers the migration of fine particles and a rapid increase in turbidity in the subballast layer. It is also observed that the hydraulic gradient at the interface is significantly higher than that within the sandy soil, indicating that contact erosion primarily occurs at the interface. Compared to static loading, cyclic loading induces significantly larger transient hydraulic gradients at both the interface and within the sandy soil. These transient hydraulic gradients allow the railway substructure, which would normally not reach the critical hydraulic gradient, to meet the hydraulic conditions necessary for contact erosion. Furthermore, the oscillating hydraulic gradients promote the reciprocating movement of pore water, creating favourable conditions for the development of seepage channels in the sandy soil. These channels accelerate the upward migration of fine particles, thereby enhancing the entire erosion process.

Limitations

As with most experimental studies, the scale of laboratory tests may not fully capture the complexities of real-world engineering problems. Consequently, further validation is needed to assess the applicability of the experimental results to field conditions. It is important to acknowledge that actual train loading conditions are highly complex, influenced by site-specific factors, operational planning, and other variables. While this study employs commonly used cyclic loading to simulate train loads, differences remain. Future research should explore the effects of load strength, frequency, and the combined forms of static and dynamic loads. Moreover, due to limitations in instrumentation, the soil used in these experiments differs from that encountered in field conditions, and the test substructures do not fully replicate actual railway configurations. These differences may result in variations in outcomes, necessitating caution when applying the findings to the selection of subgrade materials for railway embankments.

Conclusions

In this study, the focus was on investigating contact erosion in railway substructures, and a novel apparatus was developed to conduct contact erosion tests under cyclic loading conditions. Based on the experimental findings, several conclusions can be drawn:

Contact erosion occurs when the pressure head exceeds a critical value under cyclic loading. This highlights the significance of the drainage capacity of railway substructures in preventing erosion. Sandy soils with lower fines content demonstrate greater internal stability and lower particle loss from the subgrade. The critical pressure head for contact erosion is closely related to the stability of the subgrade soils.

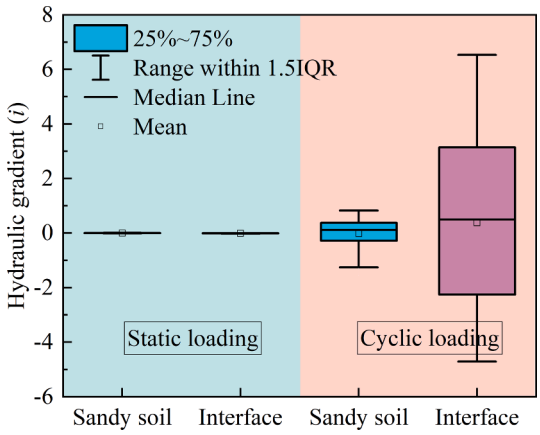

Fig. 16. Hydraulic gradient before and after application of cyclic loading.

Experimental results indicate that contact erosion in the subballast-sandy soil stratified structure leads to the migration of fine particles into the subballast layer, while the coarse eroded particles accumulate at the base, forming a low permeability interlayer. This secondary back-filter layer enhances the filter's effectiveness by reducing the likelihood of further particle migration.

The study reveals that meeting the current filter criterion commonly used in hydraulic structures does not guarantee effective prevention of contact erosion. The presence of cyclic loading can reduce the hydraulic conditions required for contact erosion to occur. Further research is necessary to investigate the geometric and hydraulic conditions for contact erosion under cyclic loading, with the aim of minimizing the risk of erosion-induced failures.

CRediT authorship contribution statement

Shaoheng Dai: Writing – original draft, Methodology, Investigation, Conceptualization. **Xuzhen He:** Writing – review & editing, Supervision, Funding acquisition. **Feng Gao:** Writing – review & editing, Methodology, Funding acquisition. **Wenhua Zhong:** Writing – review & editing, Resources, Investigation. **Yewei Zheng:** Writing – review & editing, Validation, Resources. **Sheng Zhang:** Writing – review & editing, Supervision, Project administration.

Declaration of competing interest

The authors declare that they have no known competing financial interests or personal relationships that could have appeared to influence the work reported in this paper.

Acknowledgements

This research was supported by the Australian Research Council (https://www.arc.gov.au/) Discovery Early Career Researcher Award (DECRA; DE220100763), the Young Scientists Fund of the National Natural Science Foundation of China (52308438), the science and technology innovation Program of Hunan Province (2023RC1017), the Natural Science Foundation of Hunan Province (2023JJ40035), the Open Research Fund of Science and Technology Innovation Platform of Key Laboratory of Highway Engineering of Ministry of Education (kfj2405), the Changsha Natural Science Foundation (kq2208234) and the National Engineering Research Center of Highway Maintenance Technology Open Key Fund (kfj220801).

Data availability

Data will be made available on request.

References

[1] Abeywickrama A, Indraratna B, Rujikiatkamjorn C. Excess pore-water pressure generation and mud pumping in railways under cyclic loading. In: Sundaram R, Shahu JT, Havanagi V, editors. Geotech. Transp. Infrastruct., Lecture Notes in Civil Engineering, 371–383. Singapore: Springer Singapore; 2019.

[2] Ahlinhan MF, Adjovi CE. Combined geometric hydraulic criteria approach for piping and internal erosion in cohesionless soils. *Geotech Test J* 2018;42(1): 20170096. https://doi.org/10.1520/GTJ20170096.

[3] Amiri Tasuji M, Ghadir P, Hosseini A, Javadi AA, Habibnejad Korayem A, Ranjbar N. Experimental investigation of sandy soil stabilization using chitosan biopolymer. *Transp Geotech* 2024;46:101266. https://doi.org/10.1016/j.trgeo.2024.101266.

[4] Astm. D2434-68: Standard Test Method for Permeability of Granular Soils. West Conshohocken, PA, USA: ASTM International; 2006.

[5] Aw ES. Low cost monitoring system to diagnose problematic rail bed: Case study at mud pumping site. Department of Civil and Environmental Engineering. Massachusetts Institute of Technology; 2007.

[6] Bai B, Rao D, Chang T, Guo Z. A nonlinear attachment-detachment model with adsorption hysteresis for suspension-colloidal transport in porous media. *J Hydrol* 2019;578:124080. https://doi.org/10.1016/j.jhydrol.2019.124080.

[7] Beguin R, Philippe P, Faure Y-H. Pore-Scale Flow Measurements at the Interface between a Sandy Layer and a Model Porous Medium: Application to Statistical Modeling of Contact Erosion. *J Hydraul Eng* 2013;139(1):1–11. https://doi.org/10.1061/(ASCE)HY.1943-7900.0000641.

[8] Bian X, Wan Z, Zhao C, Cui Y, Chen Y. Mud pumping in the roadbed of ballastless high-speed railway. *Géotechnique* 2022;1–15. https://doi.org/10.1680/jgeot.21.00135.

[9] Bordoloi S, Hussain R, Garg A, Sreedeep S, Zhou W-H. Infiltration characteristics of natural fiber reinforced soil. *Transp Geotech* 2017;12:37–44. https://doi.org/10.1016/j.trgeo.2017.08.007.

[10] Bruzek, R., T. D. Stark, S. T. Wilk, H. B. Thompson, and T. R. Sussmann. 2016. "Fouled Ballast Definitions and Parameters." *2016 Jt. Rail Conf.*, V001T01A007. Columbia, South Carolina, USA: American Society of Mechanical Engineers.

[11] Chang DS, Zhang LM. Extended internal stability criteria for soils under seepage. *Soils Found* 2013;53(4):569–83. https://doi.org/10.1016/j.sandf.2013.06.008.

[12] Chapuis RP, Saucier A. Assessing internal erosion with the modal decomposition method for grain size distribution curves. *Acta Geotech* 2020;15(6):1595–605. https://doi.org/10.1007/s11440-019-00865-z.

[13] Chawla S, Shahu JT. Reinforcement and mud-pumping benefits of geosynthetics in railway tracks: Model tests. *Geotext Geomembr* 2016;44(3):366–80. https://doi.org/10.1016/j.geotexmem.2016.01.005.

[14] Chen B, Liu C, Li Q, Onyekwena CC. Experimental and theoretical investigations of ground settlement around submerged defective pipelines. *Transp Geotech* 2024;101395. https://doi.org/10.1016/j.trgeo.2024.101395.

[15] Chen C, Mei S, Chen S, Tang Y, Wan C. Laboratory investigation of erosion behavior at the soil–structure interface affected by various structural factors. *Nat Hazards* 2022;111(1):1065–84. https://doi.org/10.1007/s11069-021-05070-4.

[16] "Code for Design on Subgrade of Railway (TB 10001-2005)." 2005. Beijing: Ministry of Railways of the People's Republic of China.

[17] "Code for Sub-ballast in Gravel Roadbeds of Railways (TB/T 2897-1998)." 1998. Beijing: Ministry of Railways of the People's Republic of China.

[18] Cyril G, Yves-Henri F, Rémi B, Chia-Chun H. Contact Erosion at the Interface between Granular Coarse Soil and Various Base Soils under Tangential Flow Condition. *J Geotech Geoenvironmental Eng* 2010;136(5):741–50. https://doi.org/10.1061/(ASCE)GT.1943-5606.0000268.

[19] Dai, S., X. He, C. Tong, F. Gao, S. Zhang, and D. Sheng. 2023. "Stability of sandy soils against internal erosion under cyclic loading and quantitatively examination of the composition and origin of eroded particles." *Can. Geotech. J.*, cgj-2023-0325. 10.1139/cgj-2023-0325.

[20] Dai S, Zhang S, Gao F, He X, Sheng D. Investigation of particle segregation in a vertically vibrated binary mixture: Segregation process and mechanism. *Comput Geotech* 2024;169:106236. https://doi.org/10.1016/j.compgeo.2024.106236.

[21] Ding Y, Jia Y, Wang X, Zhang J, Luo H, Zhang Y, et al. The influence of geotextile on the characteristics of railway subgrade mud pumping under cyclic loading. *Transp Geotech* 2022;37:100831. https://doi.org/10.1016/j.trgeo.2022.100831.

[22] Duong TV, Cui Y-J, Tang AM, Dupla J-C, Calon N. Effect of fine particles on the hydraulic behavior of interlayer soil in railway substructure. *Can Geotech J* 2014;51(7):735–46. https://doi.org/10.1139/cgj-2013-0170.

[23] Duong TV, Cui Y-J, Tang AM, Dupla J-C, Canou J, Calon N, et al. Investigating the mud pumping and interlayer creation phenomena in railway sub-structure. *Eng Geol* 2014;171:45–58. https://doi.org/10.1016/j.enggeo.2013.12.016.

[24] Foster M, Fell R. Assessing Embankment Dam Filters That Do Not Satisfy Design Criteria. *J Geotech Geoenvironmental Eng* 2001;127(5):398–407. https://doi.org/10.1061/(ASCE)1090-0241(2001)127:5(398).

[25] Galindo-Torres SA, Scheuermann A, Mühlhaus HB, Williams DJ. A micro-mechanical approach for the study of contact erosion. *Acta Geotech* 2015;10(3): 357–68. https://doi.org/10.1007/s11440-013-0282-z.

[26] Galindo-Torres SA, Scheuermann A, Williams D, Mühlhaus H. Micro-Mechanics of Contact Erosion. *Appl Mech Mater* 2014;553:513–8. https://doi.org/10.4028/www.scientific.net/AMM.553.513.

[27] Gao F, He X, Zhang S. Pumping effect of rainfall-induced excess pore pressure on particle migration. *Transp Geotech* 2021;31:100669. https://doi.org/10.1016/j.trgeo.2021.100669.

[28] Gao F, Zhang S, He X, Sheng D. Experimental Study on Migration Behavior of Sandy Silt under Cyclic Load. *J Geotech Geoenvironmental Eng* 2022;148(5): 06022003. https://doi.org/10.1061/(ASCE)GT.1943-5606.0002796.

[29] Guo H, Ren J, Zhang L, Kang J, Nan S, Chen K, et al. Experimental study on backward erosion piping of a double-layer dike foundation under variable exit geometries. *Transp Geotech* 2024;48:101353. https://doi.org/10.1016/j.trgeo.2024.101353.

[30] Guo Y, (Bill) Yu X. Analysis of surface erosion of cohesionless soils using a three-dimensional coupled computational fluid dynamics – discrete element method (CFD–DEM) model. *Can Geotech J* 2019;56(5):687–98. https://doi.org/10.1139/cgj-2016-0421.

[31] Han B, Cai G, Li J, Zhao C, Cui Y. Investigating particles migration caused by mud pumping in ballasted track subgrade under cyclic loading-wetting coupling. *Transp Geotech* 2022;37:100830. https://doi.org/10.1016/j.trgeo.2022.100830.

[32] Hu W, Scaringi G, Xu Q, Huang R. Internal Erosion Controls Failure and Runout of Loose Granular Deposits: Evidence From Flume Tests and Implications for Postseismic Slope Healing. *Geophys Res Lett* 2018;45(11):5518–27. https://doi.org/10.1029/2018GL078030.

[33] Indraratna B, Raut AK, Khabbaz H. Constriction-Based Retention Criterion for Granular Filter Design. *J Geotech Geoenvironmental Eng* 2007;133(3):266–76. https://doi.org/10.1061/(ASCE)1090-0241(2007)133:3(266).

[34] Indraratna B, Salim W, Rujikiatkamjorn C. *Advanced Rail Geotechnology - Ballasted Track*. CRC Press; 2011.

[35] Istomina VS. *Filtration Stability of Soils*. Moscow: Gostroizdat; 1957.

[36] Jegatheesan P, Sothilingam P, Arulrajah A, Disfani MM, Rajeev P. Laboratory Model Test on Contact Erosion of Dispersive Soil Beneath Pavement Layers. *Geotech Test J* 2015;38(6):20140179. https://doi.org/10.1520/GTJ20140179.

[37] Johnston I, Murphy W, Holden J. Alteration of soil structure following seepage-induced internal erosion in model infrastructure embankments. *Transp Geotech* 2023;42:101111. https://doi.org/10.1016/j.trgeo.2023.101111.

[38] Ke L, Takahashi A. Experimental investigations on suffusion characteristics and its mechanical consequences on saturated cohesionless soil. *Soils Found* 2014;54(4): 713–30. https://doi.org/10.1016/j.sandf.2014.06.024.

[39] Kenney, T. C., and D. Lau. 1985. "Internal stability of granular filters." 11.

[40] Kezdi. *Soil physics:selected topics*. New York, Amsterdam: Elsevier Science; 1979.

[41] Liang F, Zhang L, Wang C. An Experimental Investigation on the Mechanism of Contact Erosion in Levee Foundations Considering the Characteristics of Particle Shape and Flow Field. *J Test Eval* 2021;49(1):20190861. https://doi.org/10.1520/JTE20190861.

[42] Liu J, Zhou C. Permeability-porosity relation during erosion-induced water inrush: Experimental and theoretical investigations. *Transp Geotech* 2023;38:100893. https://doi.org/10.1016/j.trgeo.2022.100893.

[43] Liu K, Qiu R, Su Q, Ni P, Liu B, Gao J, et al. Suffusion response of well graded gravels in roadbed of non-ballasted high speed railway. *Constr Build Mater* 2021;284:122848. https://doi.org/10.1016/j.conbuildmat.2021.122848.

[44] Mehdizadeh A, Disfani MM, Evans R, Arulrajah A. Progressive Internal Erosion in a Gap-Graded Internally Unstable Soil: Mechanical and Geometrical Effects. *Int J Geomech* 2018;18(3):04017160. https://doi.org/10.1061/(ASCE)GM.1943-5622.0001085.

[45] Nguyen TT, Indraratna B. Fluidization of soil under increasing seepage flow: an energy perspective through CFD-DEM coupling. *Granul Matter* 2022;24(3):80. https://doi.org/10.1007/s10035-022-01242-6.

[46] Nguyen TT, Indraratna B, Kelly R, Phan NM, Haryono F. "MUD PUMPING UNDER RAILTRACKS: MECHANISMS. ASSESSMENTS AND SOLUTIONS" 2019;54(4).

[47] Premkumar S, Piratheepan J, Rajeev P. Contact erosion initiated by clay dispersion beneath pavement layers. *Geomech Geoengin* 2022;17(2):524–46. https://doi.org/10.1080/17486025.2020.1827161.

[48] Sherard JL, Asce F, Dunnigan LP, Talbot JR. "Basic Properties of Sand and Gravel Filters" 1984;17.

[49] Singh M, Indraratna B, Nguyen TT. Experimental insights into the stiffness degradation of subgrade soils prone to mud pumping. *Transp Geotech* 2021;27: 100490. https://doi.org/10.1016/j.trgeo.2020.100490.

[50] Tao H, Tao J. Quantitative analysis of piping erosion micro-mechanisms with coupled CFD and DEM method. *Acta Geotech* 2017;12(3):573–92. https://doi.org/10.1007/s11440-016-0516-y.

[51] Tennakoon N, Indraratna B, Rujikiatkamjorn C, Nimbalkar S. Assessment of ballast fouling and its implications on track drainage. Proc.: Conf; 2012. p. 7.

[52] Trani LDO, Indraratna B. Assessment of Subballast Filtration under Cyclic Loading. *J Geotech Geoenvironmental Eng* 2010;136(11):1519–28. https://doi.org/10.1061/(ASCE)GT.1943-5606.0000384.

[53] Tranio, L. D. O., and B. Indraratna. 2010. "EXPERIMENTAL INVESTIGATIONS INTO SUBBALLAST FILTRATION BEHAVIOUR UNDER CYCLIC CONDITIONS." 45 (3): 12.

[54] Ueng T-S, Wang Z-F, Chu M-C, Ge L. Laboratory tests for permeability of sand during liquefaction. *Soil Dyn Earthq Eng* 2017;100:249–56. https://doi.org/10.1016/j.soildyn.2017.05.037.

[55] US Army Crops Engineers. *Filter Experiments and Design Criteria: Technical Reports*. Vicksburg, Miss: Army Engineer Waterways Experiment Station; 1953.

[56] U.S. Army Engineer Waterways Experiment Station. 1941. *Investigation of filter requirements for underdrains*. 38.

[57] U.S. Department of Interior Bureau of Reclamation. Design Standards No. 13 Embankment Dams. Department of Interior Bureau of Reclamation: U.S; 2011.
[58] Wang B, Jiang Y, Zhang Q, Chen H, Liu R, Zhang Y. Cyclic shear behavior of en-echelon joints under constant normal stiffness conditions. *J Rock Mech Geotech Eng* 2024;16(9):3419–36. https://doi.org/10.1016/j.jrmge.2023.12.002.
[59] Wang B, Jiang Y, Zhang Q, Zhang Y. Cyclic shear behavior of en-echelon joints under constant normal load. *Eng Geol* 2023;325:107308. https://doi.org/10.1016/j.enggeo.2023.107308.
[60] Wen F, Li X-A, Yang W, Li J, Zhou B, Gao R, et al. Mechanism of loess planar erosion and numerical simulation based on CFD–DEM coupling model. *Environ Earth Sci* 2023;82(8):197. https://doi.org/10.1007/s12665-023-10879-2.
[61] Wilk ST, Li D. A deep investigation into the mechanisms and factors producing mud pumping of railway track. *Transp Geotech* 2023;38:100908. https://doi.org/10.1016/j.trgeo.2022.100908.
[62] Yin Z-Y, Yang J, Laouafa F, Hicher P-Y. A framework for coupled hydro-mechanical continuous modelling of gap-graded granular soils subjected to suffusion. *Eur J Environ Civ Eng* 2020;1–22. https://doi.org/10.1080/19648189.2020.1795724.
[63] Zhang S, Gao F, He X, Chen Q, Sheng D. Experimental study of particle migration under cyclic loading: effects of load frequency and load magnitude. *Acta Geotech* 2021;16(2):367–80. https://doi.org/10.1007/s11440-020-01137-x.
[64] Zhang S, Yan H, Teng J, Sheng D. A mathematical model of tortuosity in soil considering particle arrangement. *Vadose Zone J* 2020;19(1). https://doi.org/10.1002/vzj2.20004.